OXFORD

ORIGINAL ARTICLE

The Low-Threshold Calcium Channel Cav3.2 Mediates Burst Firing of Mature Dentate Granule Cells

Mael Dumenieu[1], Oleg Senkov[2], Andrey Mironov[2,3,4], Emmanuel Bourinet[5], Michael R. Kreutz[1,6], Alexander Dityatev[2,7,8], Martin Heine[9], Arthur Bikbaev[9] and Jeffrey Lopez-Rojas [ID] [1]

[1]Research Group Neuroplasticity, Leibniz Institute for Neurobiology, Brenneckestr. 6, 39118 Magdeburg, Germany, [2]Molecular Neuroplasticity Group, German Center for Neurodegenerative Diseases (DZNE), 39120 Magdeburg, Germany, [3]Lobachevsky State University of Nizhny Novgorod, 603950 Nizhny Novgorod, Russia, [4]Privolzhsky Research Medical University, 603005 Nizhny Novgorod, Russia, [5]Calcium Channel Dynamics & Nociception Group, Institute of Functional Genomics, 34094 Montpellier, France, [6]Leibniz Group "Dendritic Organelles and Synaptic Function," University Medical Center Hamburg-Eppendorf, Center for Molecular Neurobiology (ZMNH), 20251 Hamburg, Germany, [7]Center for Behavioral Brain Sciences (CBBS), 39106 Magdeburg, Germany, [8]Medical Faculty, Otto-von-Guericke University, 39120 Magdeburg, Germany and [9]Research Group Molecular Physiology, Leibniz Institute for Neurobiology, Brenneckestr. 6, 39118 Magdeburg, Germany

Address correspondence to Arthur Bikbaev. Email: artur.bikbaev@lin-magdeburg.de/Jeffrey Lopez-Rojas. Email: jeffrey.lopez@lin-magdeburg.de.

Abstract

Mature granule cells are poorly excitable neurons that were recently shown to fire action potentials, preferentially in bursts. It is believed that the particularly pronounced short-term facilitation of mossy fiber synapses makes granule cell bursting a very effective means of properly transferring information to CA3. However, the mechanism underlying the unique bursting behavior of mature granule cells is currently unknown. Here, we show that Cav3.2 T-type channels at the axon initial segment are responsible for burst firing of mature granule cells in rats and mice. Accordingly, Cav3.2 knockout mice fire tonic spikes and exhibit impaired bursting, synaptic plasticity and dentate-to-CA3 communication. The data show that Cav3.2 channels are strong modulators of bursting and can be considered a critical molecular switch that enables effective information transfer from mature granule cells to the CA3 pyramids.

Key words: axon initial segment, burst firing, Cav3.2, dentate gyrus, hippocampus, intrinsic excitability, mature granule cells, T-type calcium channels

Introduction

The dentate gyrus is the first relay station of the hippocampal trisynaptic loop and is a key structure in many hippocampus-dependent learning tasks, including contextual learning, pattern completion and pattern separation (Kesner and Rolls 2015; Lopez-Rojas and Kreutz 2016). The dentate is one of the few brain regions where adult neurogenesis occurs. Newborn, immature granule cells coexist with mature cells and are much more excitable and plastic during their maturation process than their mature counterparts (Wang et al. 2000; Schmidt-Hieber et al. 2004;

Ge et al. 2007). Therefore, immature cells have been considered the key players in dentate physiology. However, immature cells comprise only a small minority of the total granule cell population at any given time point of an adult animal lifespan. Consequently, the focus of recent research has been shifted to try to understand the physiological role of the poorly excitable and poorly plastic but majoritarian mature granule cell pool (Alme et al. 2010).

Mature granule cells are characterized by a low input resistance and a hyperpolarized resting membrane potential (Staley et al. 1992; Mongiat et al. 2009). These cells are also prominently inhibited by GABAergic innervation (Dieni et al. 2013; Temprana et al. 2015), and their dendrites impose a strong attenuation of synaptic potentials (Krueppel et al. 2011). Consequently, they only occasionally fire action potentials. More recent work has shown that besides their low spontaneous firing rate, mature granule cells in vivo fire bursts of action potentials more often than single tonic spikes (Pernía-Andrade and Jonas 2014). However, the mechanism underlying this bursting behavior is currently unknown. In general, bursts are considered to be more effective in discharging postsynaptic targets than single tonic-like spikes, which is particularly relevant for dentate-to-CA3 synapses. These synapses have a pronounced short-term facilitation and may profit more from a burst-like event than other synapses in the brain (Nicoll and Schmitz 2005). Indeed, single spikes from granule cells are rarely sufficient to trigger postsynaptic suprathreshold responses, which is in contrast to bursts of action potentials (Henze et al. 2002).

Low-threshold T-type calcium channels can open at relatively hyperpolarized membrane potentials, lower than the sodium spike threshold, thus been able to potentially influence whether and how a neuron will subsequently fire action potentials (Perez-Reyes 2003). T-type channel activation enhances excitability in thalamic neurons (Perez-Reyes 2003), and they are also present at the axon initial segment (AIS) of brainstem cartwheel cells, where they exert a strong modulatory effect on the generation of action potentials (Bender and Trussell 2009). In the dentate gyrus, immature granule cells show T-type channel-mediated low-threshold calcium spikes that reduce the current needed to elicit a sodium spike (Schmidt-Hieber et al. 2004). However, after blocking T-type channels, no changes in the action potential threshold occur in mature granule cells, and no other changes have been reported (Schmidt-Hieber et al. 2004; Martinello et al. 2015). Given that T-type channels are indeed present in mature granule cells (Martinello et al. 2015; Blaxter et al. 1989), we hypothesized that these channels, despite not affecting the action potential threshold of mature granule cells, mediate their bursting capability and are therefore a key element in achieving an efficient transmission of information from the dentate to the next synaptic relay station, the CA3 area.

Materials and Methods

All experimental procedures were carried out in accordance with the EU Council Directive 2010/63/EU and were approved by the local Committee for Ethics and Animal Research (Landesverwaltungsamt Sachsen-Anhalt, Germany).

Animals

Wistar Han rats and C57BL/6J mice, both from Charles River, were bred in-house. For local blockade of T-type channels, Wistar Han rats were ordered from Charles River and allowed to recover in house for 1–2 weeks before experiments. Cav3.2 knockout mice originally described by Chen and colleagues (Chen et al. 2003) and backcrossed to the C57BL/6J genetic background by Janvier Labs, were a kind gift from Kevin P. Campbell and were further bred in-house. Age-matched C57BL/6J mice were used as controls for the Cav3.2 knockout mice.

Single **Cell Recordings In Vitr**o

Hippocampal Slices

Transverse 400 μm slices from the right hippocampus of adult male Wistar rats (8–10 weeks old) or adult male mice (20–30 weeks old) were cut with a vibratome (Leica VT1000S) in ice-cold ACSF solution. The ACSF contained the following (in mM): 124 NaCl, 4.9 KCl, 2 $MgSO_4$, 2 $CaCl_2$, 1.2 KH_2PO_4, 25.6 $NaHCO_3$ and 20 glucose, equilibrated with 95% O_2/5% CO_2. Slices were incubated at 34 °C for 25 min and subsequently held at room temperature. The same extracellular solution was used for preparation, incubation and holding of the slices.

Current-Clamp Recordings

Patch pipettes were pulled from a horizontal micropipette puller (model P-97, Sutter Instruments) and filled with an intracellular solution containing the following (in mM): 130 potassium gluconate, 20 HEPES, 1 $CaCl_2$, 2 $MgCl_2$, and 10 EGTA. The pH was adjusted to 7.3 and the osmolarity to 290 mOsm. Pipettes of a 7–15 MΩ tip resistance were used. Once transferred to the recording chamber, slices were incubated in the bath solution for 15 min prior to recordings. The temperature in the recording chamber was adjusted to 25 °C or 32 °C for rats, depending on the experiment and as indicated in the text. For mice, all recordings were performed at 32 °C. Whole-cell patch-clamp configuration was established, and cells were held at −70 mV by injecting a small holding current. Mature granule cells were selected based on their shape, size and distribution in the 2 outer thirds of the granule cell layer. Their identity was further confirmed by their input resistance, according to the literature, below 300 MΩ (Ge et al. 2007; Wang et al. 2000; Schmidt-Hieber et al. 2004). The input resistance of the recorded cells averaged 154.3 ± 3.8 MΩ.

Characterization of Burst Firing Following Somatic Current Injection

The standard protocol to characterize the mature cell firing phenotype involved stimulating the cells with 250-ms-long depolarizing somatic current injections. We used 40 pA increasing steps starting from 0 pA with respect to the holding current. The first step eliciting firing of the cell was termed "rheobase," and the next +40 pA step was termed "rheobase+1" (R + 1). This R + 1 step was used for quantification of burst firing, as it allowed a clear discrimination between bursting and nonbursting spikes and produced consistent firing. Quantification of the burst firing was performed by measuring the interspike interval (ISI) between the first and second AP (first ISI) and later tonic spikes coming at the end of the discharge, in these conditions, the fourth and fifth AP (fourth ISI).

Except for the experiments of local puffs, all T-type channels blockers were bath-applied at the following concentrations widely used in the literature and mostly selective for T-type channels: 100 μM $NiCl_2$ (Lee et al. 1999; Bijlenga et al. 2000; Joksovic et al. 2005; Obejero-Paz et al. 2008; Engbers et al. 2012; Cui et al. 2014), 3 μM mibefradil (McDonough and Bean 1998; Martin et al. 2000; Todorovic et al. 2001; Perez-Reyes 2003), 1 μM TTA-A2 (Kraus et al. 2010; Todorovic and Jevtovic-Todorovic 2011; Francois et al. 2013; Fernández et al. 2015) and 50 μM NNC

55-0396 ([Huang et al. 2004](); [Li et al. 2005]()). NiCl$_2$ was obtained from Sigma-Aldrich, Mibefradil and NNC 55-0396 were purchased from Tocris, and TTA-A2 was a kind gift from V. Uebele (Merck). The non-T-type blockers SNX-482 and nifedipine were obtained from the Peptide Institute and Abcam, respectively.

Quantification of the Afterdepolarization and Correlation With the Firing Phenotype

Single spikes were elicited by a 5-ms-long 600 pA current injection. The amplitude of the ADP following the AP was measured at 6 ms after the peak of the AP value corresponding to the average timing of the peak of the ADP as calculated in all cells recorded for this experiment. The firing phenotype in response to the 250-ms, Δ40-pA stimulating protocol described above was also assessed in the same cells to calculate the correlation between the ADP amplitude and the first ISI at step R + 1.

Medial Perforant Path Stimulation-Driven Activity

A 6–10 MΩ patch pipette was filled with extracellular solution and placed in the molecular layer approximately 100 μm from the cell body. An ISO-Flex stimulator (A.M.P.I.) was used to deliver short square pulses of decreasing intensity from 100 to 10 μA to elicit both subthreshold and suprathreshold EPSPs. The EPSP slope and the number of spikes (which rarely exceeded 2 APs) were quantified. We estimated the threshold EPSP slope values, the values of EPSP slope eliciting spikes with 50% probability, individually for each cell from their E-S curves relating the EPSP slopes with the spiking probability for "1 AP and more" or "2 APs and more." The extracellular solution contained 20 μM bicuculline.

Local Blockade of T-Type Channels

For these experiments, 100 μM Alexa594 was added to the intracellular solution to allow visualization of granule cell processes. The extracellular solution was the same as described previously, except that KH$_2$PO$_4$ was removed to prevent NiPO$_4$ precipitation and that KCl was increased to 6.1 mM to compensate for it. The extracellular solution contained 10 μM CNQX, 50 μM D-AP5 and 20 μM bicuculline. A 100–130 MΩ tip resistance patch pipette was filled with extracellular solution and contained 10 mM NiCl$_2$ and 100 μM Alexa594—or only extracellular solution and 100 μM Alexa594 for the control group—and was mounted on a micropressure system from npi electronic (Tamm, Germany). Alexa594 fluorescence was used to ensure that no solution was leaking from the puff pipette as well as to estimate the size of the puff, which encompassed an area of approximately 5–25 μm diameter.

Following the establishment of the whole-cell configuration, the position of the axon and proximal dendrites were quickly assessed using Alexa594 fluorescence. The puff pipette was then placed in close proximity to the axon or a proximal dendrite, 20 μm away from the soma. Granule cells were then stimulated with 250-ms-long depolarizing steps of somatic current injections (R + 1) ± 20 pA. After 4 repeats, 15-PSI pressure steps of 100 ms increasing length, starting from 100 ms up to 800 ms and ending at the beginning of the somatic current injection stimulation, were applied through the micropressure system paired with 8 repeats of the somatic current injection protocol. The somatic injection protocol was then repeated every 15 s until a stable recovery of the burst firing. The speed of recovery was variable, ranging from seconds to a couple minutes, but it mostly occurred within a minute.

Two-Photon Imaging

A commercial 2-photon laser-scanning Femto2D microscope from Femtonics (Budapest, Hungary) was used. Laser pulses at 810 nm were provided by a Ti:Sapphire femtosecond laser (Cameleon Ultra I, Coherent). For measuring Ca^{2+} signals, green (Fluo-5F) and red (Alexa-Fluor 594) fluorescence values were collected during 500 Hz line scans. Fluorescence changes were quantified as the increase in green fluorescence normalized to the average red fluorescence (ΔG/R) ([Yasuda et al. 2004]()). The Ca^{2+} transient peaks were estimated from exponential fits of the fluorescence traces. Fluorescence was collected through the objective (60 × 1.0 NA, Olympus) and the oil immersion condenser (1.4 NA, Olympus) with 2 pairs of photomultipliers (2 for collecting red band fluorescence and the other 2 for green band fluorescence). An additional photomultiplier was used to collect the transmitted infrared light. The composition of the intracellular solution for these experiments was as follows (in mM): 130 potassium gluconate, 20 HEPES, 2 MgCl$_2$, 2 Mg-ATP, 0.3 Na-GTP, 0.25 Fluo-5F and 0.02 Alexa594. The pH was adjusted to 7.3 and the osmolarity to 290 mOsm. The extracellular solution was the same as in the other experiments and contained 20 μM bicuculline. Fluorescence data recording started 15 min after obtaining the whole-cell configuration.

Granule cells were stimulated with two 5-ms-long current injections of 600 pA intensity to elicit a doublet of APs at 50 Hz that reliably propagated to distal dendrites and axon. In another protocol, APs were blocked by bath application of 1 μM TTX, and cells were stimulated with current injections that were 250 ms in length and had a 40 pA increasing intensity to reproduce the standard protocol used to characterize burst firing. Care was taken to not depolarize the cells further than −20 mV, providing maximal T-type channel activation with limited activation of high-voltage-activated calcium channels ([Perez-Reyes 2003](); [Pourbadie et al. 2017]()). This protocol produced membrane potential changes that could not propagate reliably to distal processes and was used to assess T-type channel-mediated fluxes in the proximal axon more specifically.

Field Recordings In Vitro

Hippocampal Slices

Field recordings were done in transversal hippocampal slices from 20- to 30-week-old male mice. The right hippocampus was isolated in ice-cold ACSF solution. Hippocampal slices (400 μm thickness) were cut with a chopper and placed in an interface chamber at 32 °C. The ACSF solution was the same as that in the single-cell experiments. Slices were incubated for at least 3 h before the start of the recordings, which were performed in the same incubation interface chamber at 32 °C ([Sajikumar et al. 2005]()).

Electrophysiology

The population spikes and the field-excitatory postsynaptic potentials were measured with 2 monopolar lacquer-coated, stainless steel electrodes positioned at the granule cell layer and middle of the molecular layer. One stimulation electrode placed in the middle of the molecular layer was used to stimulate the medial perforant path. Biphasic constant current pulses (0.1 ms per half-wave duration) to the perforant path at 0.033 Hz evoking 25% of maximal population spike amplitude were used for test recordings.

LTP-Induction Protocol

The LTP-induction protocol was theta-burst stimulation (TBS) and consisted of 4 episodes repeated at 0.1 Hz; each episode included brief presynaptic bursts, that is, 10 pulses (0.2 ms per half-wave duration, with the same stimulation intensity as in baseline recordings) at 100 Hz, repeated 10 times at 5 Hz.

In **Vivo Reco**rdings

Headstages and Tetrodes

Tetrodes consisted of 4 wires twisted together (Formvar-coated Nichrom wire ∅18 μm/25 μm, Science Products) using a magnetic stir for spinning and glued as one tetrode by melting Formvar with a heating gun. Headstages were self-designed to house 8 tetrodes and one 32-channel EIB (Electrode Interface Board, Neuralynx). The whole implant, including 3D printed parts, EIB, tetrodes, pins, screws and copper adhesive tape around the headstage weighed approximately 3–4 g.

Implantation

Chronic implantation of tetrodes in mice was performed similarly as in previous work (Senkov et al. 2015, 2016), with minor changes. In brief, mice were anesthetized with 1–3% isoflurane delivered as a mixture with O_2 through a vaporizer (Matrx VIP 3000, Midmark) and a mouse breathing mask. The mice were placed in a stereotaxic frame (Narishige, Japan), on a heating pad (DC Temperature Controller, WPI) to maintain a constant mouse body temperature (34–36 °C) during surgery. Coordinates for 8 tetrodes, for 4× tetrodes in the mouse dorsal hippocampal dentate gyrus in both hemispheres, were as follows: AP: −1.6 mm, L: ±0.75–1, DV: 2.0 mm; and AP: −2.5 mm, L: ±1.5–2, DV: 2.0 mm; and for 4× tetrodes in the CA3 area of the hippocampus in both hemispheres: AP: −1.6 mm, L: ±1.5–1.75, DV: 2.0 mm; and AP: −2.5 mm, L: ±2.5–3, DV: 2.25–2.5 mm, were set according to the mouse brain atlas (Paxinos and Franklin 2012).

After the surgery lasting for approximately 4–5 h, the mice were placed back into their home cages and monitored until full awakening. Carpofen (5 mg/kg b.w. s.c., Rimadyl, Pfizer Pharma GmbH) was used as a postoperative analgesic. All recordings were performed after the mice had fully recovered, usually at 2–3 weeks. Recordings were done by using a Neuralynx 32-channel preamplifier and a 5-m tether. Two rolling blocks helped to reduce the weight of the implant and the cable.

Local Field Potential and Unit Activity Recordings

Intrahippocampal local field potentials (LFPs) were recorded using a digital electrophysiological 64-channel recording system (Neuralynx, USA) and data acquisition software Cheetah (Neuralynx, USA). Multi-unit activity was sampled at 32 KHz with a wide-band 0.1 Hz–10 kHz range filter. Animals were exposed to a novel context and allowed to freely explore it while neural activity was recorded. The recording session lasted for 5 min. At the end of the recording session, mice were sacrificed, and the position of the tetrodes was verified. Only tetrodes with a correct position were selected for further analysis.

LFP Analysis

Treatment and processing of signals were carried out in off-line mode using Spike2 software (Cambridge Electronic Design, UK). To remove the 50 Hz AC noise, original wide-band recordings of the network activity with a sampling rate of 32 kHz were processed using forward fast Fourier transform (FFT); the power of the 50 Hz component and its harmonics was set to 0, and the inverse FFT was applied to reconstruct the signals. Obtained records were low-pass filtered (350 Hz), down-sampled to 1 kHz (factor 32) and used for further analysis of the theta and gamma oscillatory activity. For analysis of the network oscillations in the theta (5.0–12.5 Hz) and gamma (30.0–100.0 Hz) frequency bands, LFP signals in individual electrodes were integrated for each tetrode in each animal. The spectral power of oscillatory components in the frequency range 0–500 Hz was obtained using sliding FFT (2^{11} points in 2.048 s epochs, Welch's method).

Units Activity Analysis

Action potentials were detected in a bandpass filtered signal (0.5–10.0 kHz). Events within a window of 1.25 ms (40 points at 32 kHz) with a magnitude exceeding 6 standard deviations above the mean were detected, and spike waveforms were extracted and stored for further classification. Spike sorting using principal component analysis (PCA) was followed by visual inspection and manual adjustment of clusters if necessary. Later, the mean firing rates for classified units in the DG and CA3, as well as bursting properties for units in the DG with a mean bursting rate ≥0.5 burst/min, were computed. Units with a mean firing rate <0.05 Hz were considered inactive and discarded from the analysis. The following burst criteria were used: number of spikes ≥2, maximal intraburst ISI ≤15 ms. Finally, the spike shapes of obtained units were visually inspected, and inhibitory neurons were identified based on their higher firing rate (generally above 10 Hz) and shorter latency compared with respective values in principal cells. Throughout the text, the data only for putative excitatory neurons are presented.

Experimental Design and Statistical Analysis

Experiments reported in this study were designed to examine the effect of pharmacological blockade or genetic ablation of T-type channels on the firing pattern and calcium influx in mature granule cells of adult male rodents, as well as to characterize the implications of these changes on dentate gyrus synaptic plasticity and dentate-to-CA3 communication. All data are presented as the mean±standard error of the mean. For statistical analysis, the normality of the data sets was assessed with the D'Agostino & Pearson omnibus normality test prior to further parametric or nonparametric tests, as indicated in the text. Statistical tests were performed with Prism 6 (GraphPad Software, Inc., La Jolla, CA).

Results

T-Type Calcium Channels Mediate Burst Firing of Mature Granule Cells

We first studied the firing pattern of mature granule cells ($n = 25$) after somatic current injection. Interestingly, the firing pattern elicited by small current injections followed a stereotypical pattern. The first 2 action potentials of the discharge were closer to each other in time than were the rest of the action potentials that were more evenly distributed: a burst of few action potentials followed by tonic spikes later on (Fig. 1A). The frequency of the burst was approximately 50 Hz (17.94 ± 1.70 ms), much higher than the frequency of the subsequent tonic spikes (fourth ISI, ISI: 41.07 ± 2.50 ms, approximately 24 Hz).

We next asked whether pharmacological blockade of T-type channels might impact the firing pattern of mature granule
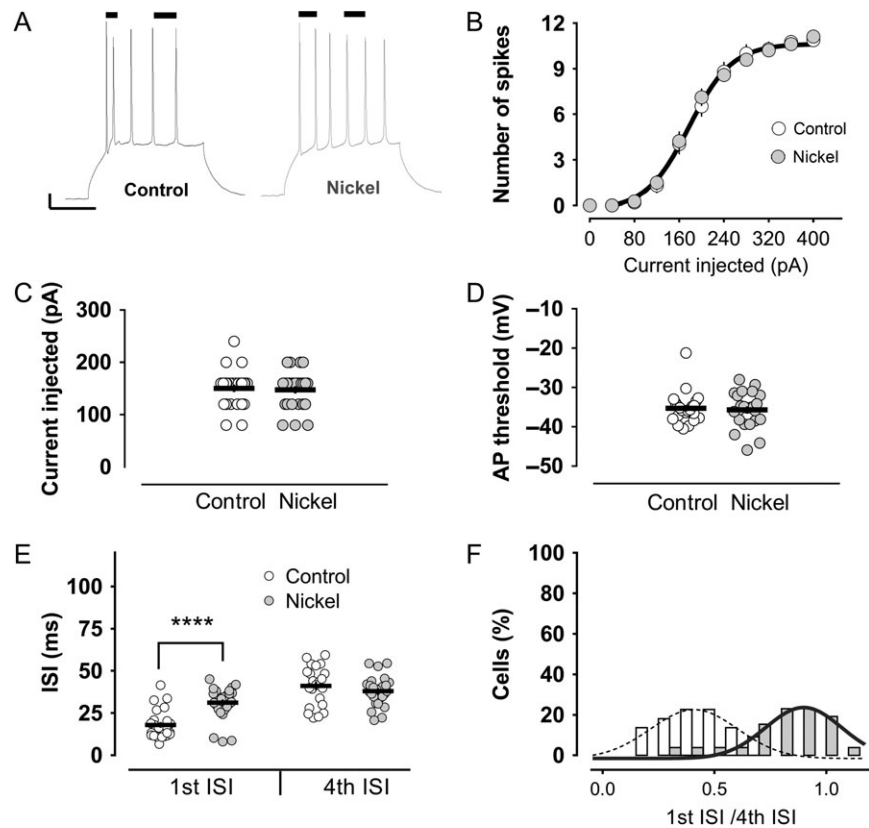
Figure 1. The stereotypical firing of mature granule cells, but not their general excitability, is modified by nickel, a T-type channel blocker. (A) A representative trace shows the characteristic firing pattern of mature granule cells in response to a square pulse current injection to the soma, specifically, an early burst of spikes, followed by tonic action potentials. Also shown is an illustrative trace of the discharge in the presence of 100 μM nickel in the bath. The bars on top of the traces indicate the first and fourth ISIs. Scale bars: 10 mV/100 ms. Nickel did not modify the general excitability of the mature granule cells. Neither the number of action potentials (B), nor the minimum current needed to elicit an action potential (i.e., rheobase) (C), nor the action potential threshold (D), were modified by nickel. (E) There was, however, a strong impairment of the burst firing by nickel, with no modification of the later tonic spikes. (F) The effect of nickel is clearly appreciated as a shift in the distribution of the "first ISI/fourth ISI" ratios to a value close to 1 (0.81). In the control group, the ratio was 0.43. Both ratios were significantly different ($P < 0.0001$, Mann–Whitney U-test.). ****$P < 0.0001$, Mann–Whitney U-test.

cells. To this end, we recorded from a group of cells ($n = 26$) perfused with an extracellular solution containing 100 μM nickel, a classical T-type calcium channel blocker. In agreement with previous studies (Schmidt-Hieber et al. 2004; Martinello et al. 2015), nickel did not change the general excitability of the mature granule cells. The number of action potentials, the action potential threshold and the current needed to elicit action potentials were indistinguishable among the control and the nickel-treated groups (Fig. 1B–D). What was changed, however, was the pattern of the discharge. All spikes in the presence of nickel were generated in a rather similar tonic-like fashion (first ISI: 31.12 ± 1.89 ms and fourth ISI: 38.00 ± 1.69 ms) (Fig. 1E). The nickel effect was also reflected in the frequency distribution of the ISI ratios (first ISI/fourth ISI): most of the cells had a ratio close to 1 (first ISI/fourth ISI ratio: 0.81 ± 0.037), typical of a tonic firing mode. This is in contrast to the cells recorded in the control group, where the ratio was twice lower (first ISI/fourth ISI ratio: 0.43 ± 0.033), reflecting the difference in the intervals for the bursting and nonbursting spikes (Fig. 1F).

To confirm these results and to rule out any unspecific effects of nickel, we repeated the experiments in the presence of 3 other T-type channel blockers: mibefradil 3 μM ($n = 20$), NNC 55-0396 50 μM ($n = 19$) and TTA-A2 1 μM ($n = 18$). Convincingly, the effects of all the blockers were very consistent: a strong influence on the bursting behavior with no
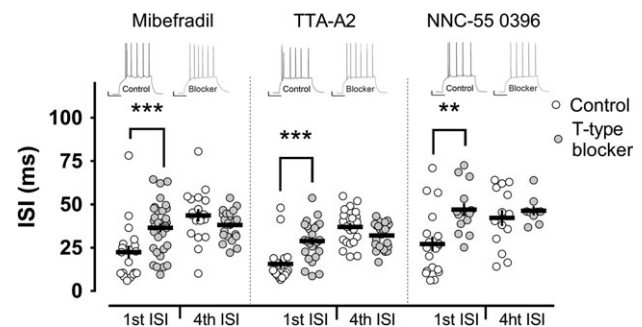

Figure 2. T-type calcium channels mediate burst firing in mature granule cells. Burst firing was impaired by bath application of different T-type channel blockers: Mibefradil, TTA-A2 and NNC-55 0396. These blockers, similarly to nickel, profoundly affected the first ISI, with no significant modification of the tonic spikes (fourth ISI). Insets show representative examples of electrophysiological traces in the corresponding groups. Scale bars: 10 mV/100 ms. **,***$P < 0.01$, $P < 0.001$ Mann–Whitney U-test.

significant changes in general excitability (Fig. 2). The ISI of the first 2 action potentials (burst in control conditions) was increased by more than 10 ms in all treated groups, making their instantaneous frequency close to the frequency of the tonically generated action potentials in the discharge (Fig. 2).

Burst Firing Relies on Intrinsic T-Type Calcium Channels and Does not Directly Relate to the Action Potential Afterdepolarization

Since T-type calcium channels are present at synapses (Weiss and Zamponi 2013; Ly et al. 2016), we sought to test the hypothesis that the effects of the T-type channel blockers on bursting were due to changes in intrinsic properties of mature granule cells and not to alterations in the network (i.e., feedback GABAergic inhibition or other). We therefore pharmacologically isolated granule cells from their network by blocking NMDA (50 μM D-AP5), AMPA/KA (10 μM CNQX) and GABA$_A$ (20 μM bicuculline) receptors. Pharmacological blockade of T-type channels with nickel (n = 23), mibefradil (n = 28), NNC 55-0396 (n = 20), or TTA-A2 (n = 34) under these conditions still led to a significant increment in the first ISI with no consistent effects on the tonic spikes (Supplementary Fig. S1). For instance, nickel increased the ISI of the bursting spikes to 27.24 ± 2.79 ms, a value significantly higher than in control conditions (16.73 ± 1.91 ms), while very close to the ISI of the tonic spikes in control (30.86 ± 2.79 ms) or nickel (31.03 ± 1.81 ms) groups. The next series of experiments were performed in the presence of this cocktail of synaptic blockers unless otherwise indicated.

Action potential afterdepolarization is an intrinsic phenomenon that has been related to the burst firing of CA1 pyramidal cells (Metz et al. 2005). We therefore explored the possibility that the afterdepolarization also affected the bursting of mature granule cells. To this end, we quantified the action potential afterdepolarization in control conditions and when T-type channels were blocked with nickel (n = 21), TTA-A2 (n = 42) or NNC 55-0396 (n = 17). We did not find any significant modification of the afterdepolarization by any of the blockers (Supplementary Fig. S2A), in contrast to previous experimental evidence showing that T-type channels might contribute to the ADP in immature granule cells (Zhang et al. 1993). We also did not find any significant correlation between the afterdepolarization amplitude and the strength of the burst, quantified as the ISI of the bursting spikes, in control cells (n = 76) (Supplementary Fig. S2B). Since it was reported that R-type channels contribute to the afterdepolarization and burst firing of CA1 pyramidal cells (Metz et al. 2005) and R-type currents can be recorded in granule cells (Sochivko et al. 2002), we also tested the effect of R-type channels blockade by 500 nM SNX-482 (n = 18) on the bursting behavior of mature cells. SNX-482 is a potent blocker of Kv4.3 A-type potassium channels that also blocks R-type calcium channels (Newcomb et al. 1998; Bourinet et al. 2001; Kimm and Bean 2014) with a variable efficacy among cell types (Newcomb et al. 1998). We chose a concentration of SNX-482, which was previously shown to be effective in granule cells (Sochivko et al. 2002; Breustedt et al. 2003). We found that R-type channel blockade did not significantly influence the bursting behavior of mature granule cells (Supplementary Fig. S2C). Collectively, these data point to a distinct intrinsic mechanism of burst firing in mature granule cells that does not involve action potential afterdepolarization.

T-Type Channels at the AIS Control the Burst Firing of Mature Granule Cells

Based on these results, we concluded that T-type channels are important contributors to burst firing in mature granule cells and that bursting is an intrinsic property of these cells. We next tried to address the spatial distribution of the burst-relevant T-type calcium channels in mature granule cells.

First, we measured calcium influx along axon and dendrites of mature granule cells (Fig. 3A) in control conditions (n = 29) and in the presence of T-type channel blockers (Mibefradil n = 20, NNC 55-0396 n = 6) after making the cells fire a doublet of action potentials at 50 Hz, a frequency similar to the one that we recorded for the bursting spikes in the previous experiments. We observed putative T-type-mediated calcium influx all along the dendrites, with a trend toward a larger influx with increasing distance to the soma (Fig. 3B). In axons, a different pattern appeared, with a much larger component in the proximal axon (Fig. 3C). The proximal axon is a region of utmost importance for the generation of action potentials (Debanne et al. 2011; Yamada and Kuba 2016); therefore, we further investigated this issue. In the subsequent experiment, we used steps of current injection similar to the ones used when assessing the effect of the T-type blockers on burst firing. Furthermore, we blocked action potentials to obtain a smaller depolarization that would render a more accurate estimation of the spatial distribution of the calcium influx (Gabso et al. 1997; Sabatini et al. 2002). Interestingly, under these conditions, T-type calcium influx was limited to the 15–30 μm of the proximal axon (Fig. 3D, control group n = 6, nickel group n = 8). This region overlaps with the region of the mature granule cell axon where action potentials are generated (Schmidt-Hieber and Bischofberger 2010), namely, the AIS.

We next tried to distinguish whether T-type channels at dendrites or AIS of mature granule cells were responsible for their bursting phenotype by local puff application of nickel. Local blockade of T-type channels on dendrites did not significantly affect the ISI of bursting spikes, whereas local blockade of T-type channels at the level of AIS significantly increased the ISI of the first 2 spikes to 2- to 3-fold the control baseline values (Fig. 3E; nickel to dendrites, n = 4; vehicle to AIS, n = 4; and nickel to AIS, n = 7). The effect was reversible, and the burst firing usually recovered after a couple of minutes. By puffing nickel on the AIS, we also observed a slight change in the action potential threshold (Fig. 3F). Nevertheless, as we did not observe any significant modifications of the action potential threshold or general excitability of mature granule cells by applying the T-type blockers in the bath, nor have others reported such changes (Schmidt-Hieber et al. 2004; Martinello et al. 2015), these changes in the first action potential threshold might have been caused by the higher, and therefore less specific, concentrations of nickel used in the local puffing. Nickel may indeed block high-voltage calcium and sodium channels at high concentrations (Yamamoto et al. 1993).

High-Frequency Burst Firing in Mature Granule Cells is Also Mediated by T-Type Channels at Near-Physiological Recording Temperature

The mean intraburst frequency of the action potentials we observed in control conditions at 25 °C was approximately 50 Hz. However, mature granule cells can fire bursts of more than 150 Hz in vivo (Pernía-Andrade and Jonas 2014). As temperature modifies T-type channel properties (Iftinca et al. 2006) and because T-type channels mediate burst firing in mature granule cells, we hypothesized that such high-frequency burst firing could be found at higher temperatures. Indeed, recording at 32 °C increased the mean intraburst frequency of mature granule cells up to 140 Hz (Supplementary Fig. S3). When recording at 32 °C, it also became apparent that often, more than 2 spikes occurred within the bursts, and frequently,
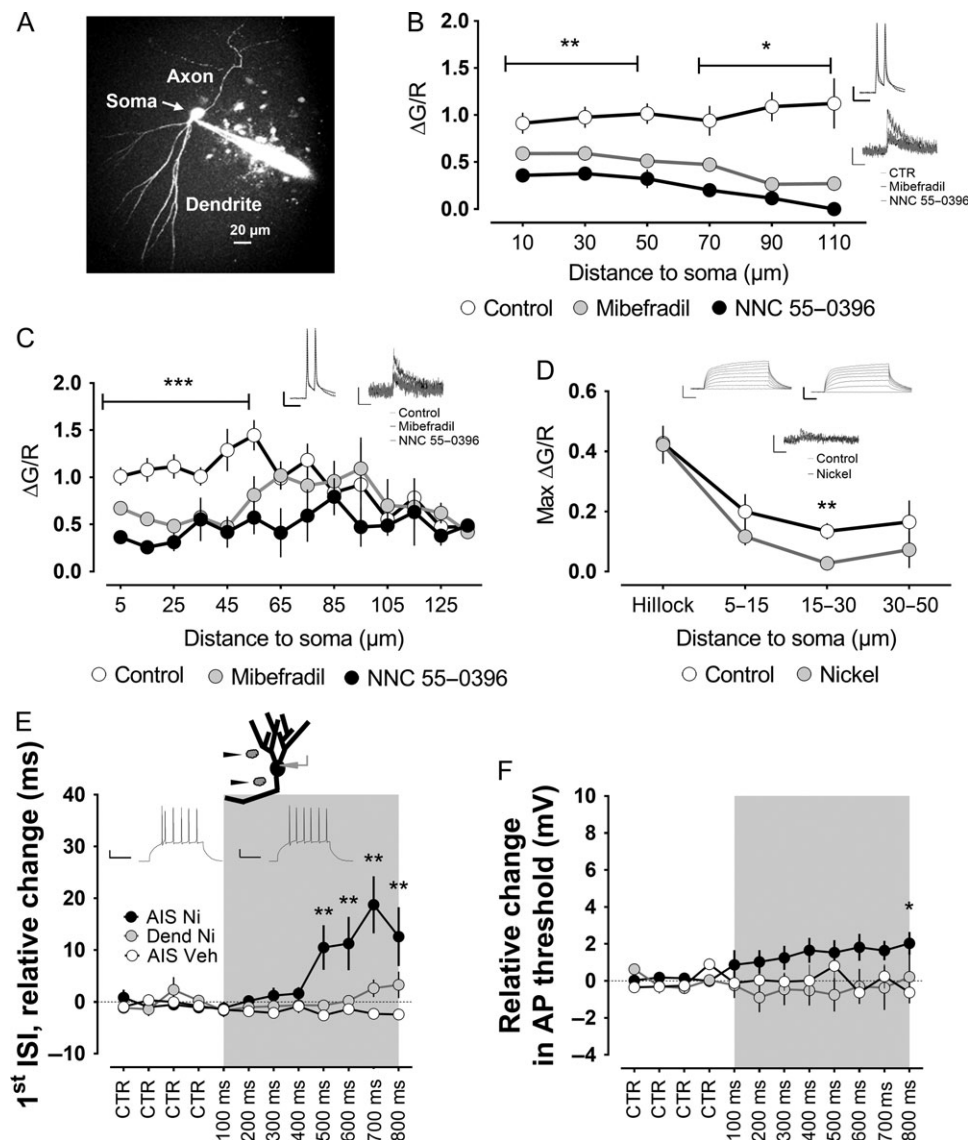
Figure 3. T-type channels at the level of the axon initial segment mediate burst firing of mature granule cells. (A) Two-photon fluorescent image of a mature granule cell filled with Alexa594, as a volume marker, and the calcium indicator Fluo-5F. (B) The cells received short pulses of current injection to the soma to evoke a doublet of action potentials at 50 Hz, as shown in the inset. T-type channel blockers mibefradil and NNC-55 0396 caused a significant reduction in the doublet-evoked calcium influx all along the recorded dendrites. In the axon, however, the effect was stronger in the proximal part (C). Insets show examples of electrophysiological and calcium influx traces in the corresponding groups for the proximal axon and dendrite. Scale bars: 20 mV/50 ms, 0.5 dG/R/500 ms. (D) To further understand the spatial distribution of the T-type-mediated calcium influx into the proximal axon, we blocked action potentials with TTX and used a longer current injection similar to the one used in a previous series of experiments. A significant effect of the T-type channel blocker nickel was only verified at a distance of 15–30 μm from the soma. Insets show examples of electrophysiological and calcium influx traces. Scale bars: 20 mV/50 ms, 0.5 dG/R/500 ms. (E) Nickel or vehicle solution was puffed at dendrites or the axon initial segment, as indicated. For each cell, 4 repeats were taken as the baseline (CTR), and puffs of increasing duration, from 100 up to 800 ms, were then applied at the specified locations. Applying nickel locally to dendrites did not significantly modify the bursting, quantified as the first ISI. In addition, there was no significant effect of local application of vehicle solution to the axon initial segment of mature granule cells. However, puffing nickel at the axon initial segment produced a highly significant increase in the first ISI. The traces in the inset show the pattern of action potentials in the control condition (left) or when puffing nickel to the AIS (right). Scale bars: 20 mV/100 ms. (F) In addition to the strong effect on the burst firing, the puff of nickel at the axon initial segment also slightly increased the threshold of the action potential, although it only reached statistical significance for the longest puff. *,**, ***$P < 0.05$, $P < 0.01$, $P < 0.001$, Mann–Whitney U-test.

multiple bursts appeared in the discharge, which might be an indication of the faster recovery rate from inactivation of T-type channels and their larger conductance at higher temperatures (Iftinca et al. 2006).

Next, we proceeded to verify the T-type channel dependence of this bursting phenotype. Both T-type blockers, nickel ($n = 8$) and TTA-A2 ($n = 8$), significantly increased the first ISI, corresponding to the more reliable bursting event in the discharge, without significant modification of the later tonic fourth ISI. With both blockers, the intraburst frequency was decreased by approximately 3-fold, from 140 Hz in the control group to approximately 45 Hz in the presence of the blockers. This frequency was again very close to the frequency of the later tonic spikes in control and treated conditions, that is, approximately 40 Hz in all cases (Supplementary Fig. S3).
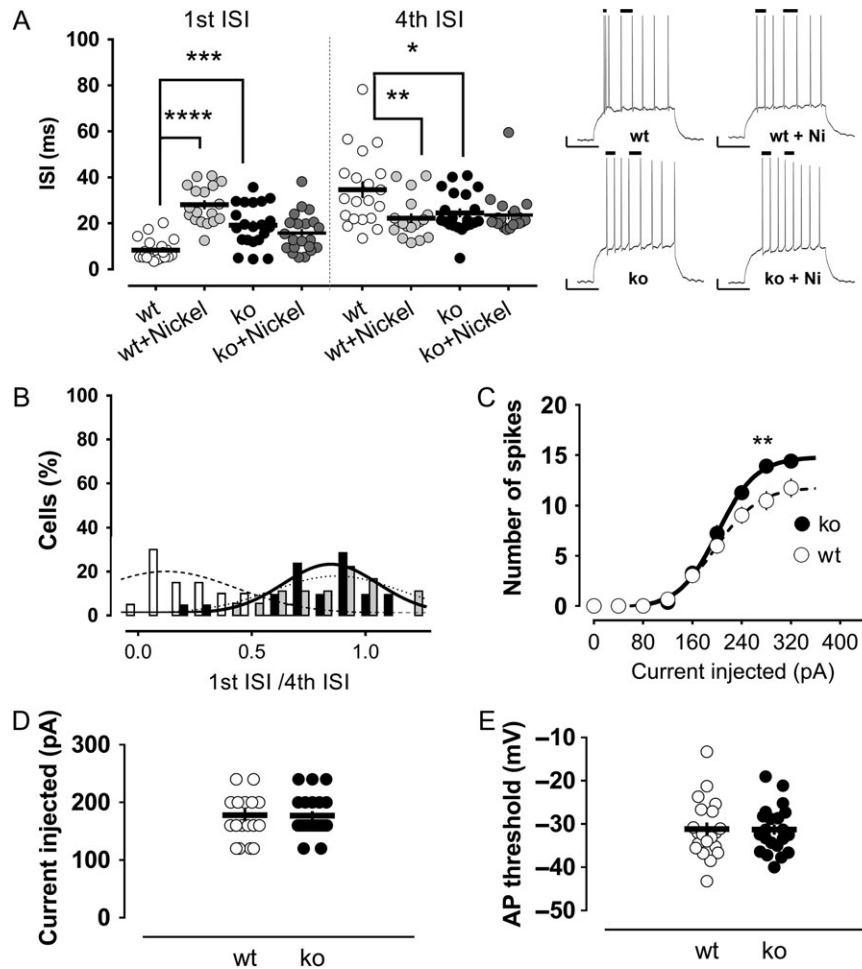
Figure 4. Burst firing of mature granule cells is conserved in mice and is mediated by the Cav3.2 T-type channel subtype. (A) Murine mature cells fire high-frequency bursts of action potentials that are strongly impaired in the presence of the T channel blocker nickel or in animals lacking the Cav3.2 channel subtype (Cav3.2 knockout). The first ISI, corresponding to the burst spikes in control conditions, is significantly increased in the nickel and the Cav3.2 knockout groups compared with the control animals. There was also a significant decrease in the fourth ISI in these groups. Nickel did not significantly modify the first or fourth ISI in the Cav3.2 knockout mice. Insets show illustrative traces of the pattern of action potentials in the different groups. The bars on top of the traces indicate the first and fourth ISIs. Scale bars: 10 mV/100 ms. (B) The effect of nickel or Cav3.2 channels knockout is clearly appreciated in the significant shift of the distribution of the "first ISI/ fourth ISI" ratios to values closer to 1 (0.85 and 0.78 in the nickel and knockout groups, respectively). In the control group, the ratio was 0.30. General excitability was not affected in the Cav3.2 knockout mice compared with the wild-type animals. Neither the number of action potentials (C), the minimum current needed to elicit an action potential (D), nor the action potential threshold (E), were modified in the absence of the Cav3.2 T-type channel subtype. *,**,***,****$P < 0.05$, $P < 0.01$, $P < 0.001$ and $P < 0.0001$, Mann–Whitney U-test.

T-Type-Mediated Mature Granule Cells Burst Firing is Present in Rats and Mice and is Mediated by Cav3.2

All previous experiments were performed in young adult rats. The pattern of discharge in response to somatic current steps in mice was quite similar to the one in rats. Very often, a high-frequency burst was observed, more frequently in the first part of the discharge, though sometimes multiple bursts were seen, followed by a more tonic arrangement of the later spikes. As in rats, blocking T-type channels with nickel ($n = 18$) significantly modified the firing pattern of mature granule cells in mice. Nickel increased the first ISI by approximately 3-fold. The intra-burst frequency changed from 120 Hz in the control group to 35 Hz in the presence of nickel (Fig. 4A).

Next, we sought to identify the T-type channel subtype responsible for the burst firing in mature granule cells, taking advantage of the available knockout lines. For this purpose, we recorded from mature granule cells of mice lacking the Cav3.2 channel ($n = 21$). The first ISI was increased by 2- to 3-fold in Cav3.2 knockout animals compared with the values of the control group (Fig. 4A). Remarkably, the firing pattern in the absence of Cav3.2 closely resembled the pattern observed in the control mice in presence of nickel. Thus, in both of these conditions of impaired T-type function, the frequency distribution of the ratios "first ISI/fourth ISI" was shifted to high values close to unity, characteristic of a tonic firing mode. In contrast, in the control group, the ratios had a distribution much closer to 0.1–0.2, reflecting the difference in the intervals for the bursting and nonbursting spikes (Fig. 4B).

Notably, apart from the impairment in burst firing, the general excitability in Cav3.2 knockout mice was indistinguishable from that of the control animals. The number of spikes, the required current to elicit an action potential and the action potential threshold were not different between these groups (Fig. 4C–E).
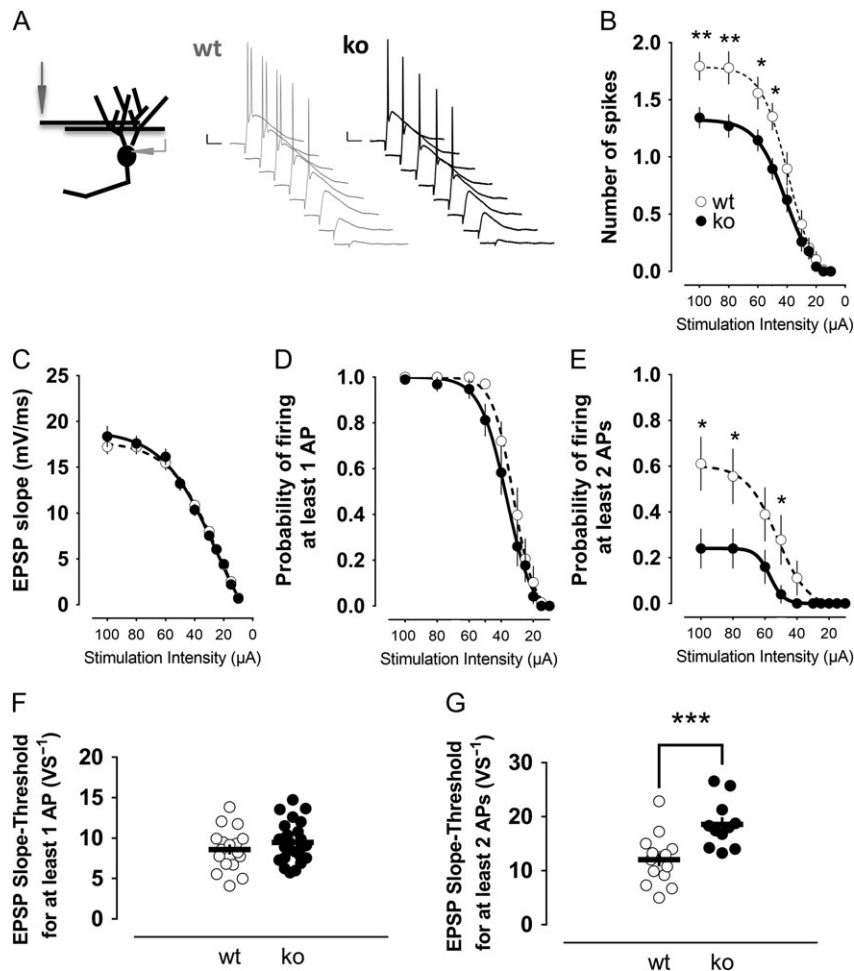
Figure 5. Ability of mature granule cells to fire doublets of action potentials in response to synaptic stimulation is greatly impaired in Cav3.2 knockout mice. (A) The medial perforant path was stimulated, and the evoked activity was evaluated in mature granule cells from wild-type and knockout animals. A decreasing series of stimulation intensities was applied. Representative traces of evoked potentials from wild-type mature granule cells and Cav3.2 knockout mature cells are shown. Scale bars: 10 mV/20 ms. (B) The number of action potentials elicited was significantly decreased in knockout animals, especially at intensities higher than 50 μA. (C) The synaptic strength, quantified as the slope of the EPSP, was not different between the groups. (D) The ability of the cells to fire *per se* was not changed by the absence of Cav3.2. E, The cells from knockout mice had an impaired ability to fire more than one action potential, which was especially the case at intensities higher than 50 μA. These results were confirmed by the comparison of the EPSP slopes required to fire per se (F) or to fire bursts of action potentials (G). *,**,***P < 0.05, P < 0.01 and P < 0.001, Mann–Whitney U-test.

These results point to Cav3.2 as the main T-type channel subtype mediating the burst firing in mature granule cells, a fact that is reinforced by the lack of a further effect of nickel on the bursting ISI of Cav3.2 knockout mice (Fig. 4A).

"Synaptically Driven Bursting" is Also Impaired in Cav3.2 Knockout Mice

Since neurons receive their inputs through synapses, we sought to further evaluate whether the ability to fire bursts was also compromised in Cav3.2 knockout mice upon synaptic stimulation. For this purpose, we stimulated the medial perforant path and looked for potential differences between mature granule cells of Cav3.2 knockouts (n = 25) and control mice (n = 18) (Fig. 5A). We observed that the number of spikes elicited was reduced in knockout animals (Fig. 5B). Since the excitatory input—measured as the slope of the excitatory postsynaptic potential—was practically identical between the groups (Fig. 5C), the results suggest that the intrinsic ability of the cell to fire was impaired in knockout mice. Next, we aimed to

dissect whether the apparent impairment was due to a general compromised ability of granule cells to fire or if there was a specific deficiency in eliciting bursts (2 or more spikes). Remarkably, while the probability of firing per se (quantified as the probability to fire at least one action potential) was not significantly changed in the knockout animals (Fig. 5D), we observed that the probability of firing 2 or more action potentials was reduced (Fig. 5E). Accordingly, the excitatory input needed to fire at least one spike with 50% probability was not significantly different between both genotypes (Fig. 5F), whereas the excitatory postsynaptic potential slope required to fire 2 or more action potentials with 50% probability was increased by almost 2-fold in the knockout mice (Fig. 5G).

We confirmed these results by recording evoked field potentials after medial perforant path stimulation (Supplementary Fig. S4). As in single-cell recordings, the field-EPSP slope (Supplementary Fig. S4A) as well as the ability to fire per se (Supplementary Fig. S4B) was similar between wild-type and knockout mice. Thus, the E-S curves relating the field-EPSP slopes to the first spike amplitudes were essentially identical,
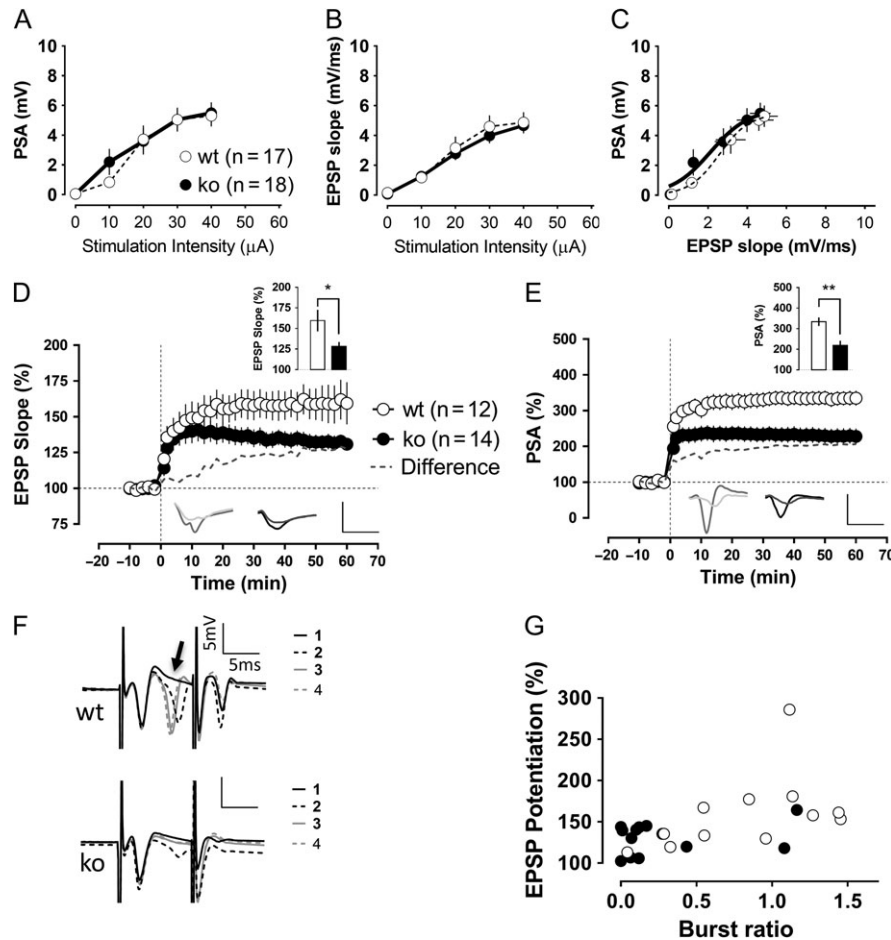
Figure 6. Impaired dentate gyrus synaptic plasticity in Cav3.2 knockout mice. Recordings of evoked field potentials were made after stimulation of the medial perforant path. General excitability and synaptic transmission seemed to be unaffected in knockout animals, as shown in the similar population spike amplitudes (A), EPSP slopes (B) and the EPSP slope relation to the generation of action potentials (C). However, the level of synaptic potentiation recorded 1 h after the TBS was reduced in the knockout group compared with control animals ($P < 0.05$, Mann–Whitney U-test). In (D and E), the potentiation levels of the field-EPSP and population spike after the TBS protocol are shown. The insets show the potentiation level in the last 10 min of recordings as well as traces corresponding to baseline and 1 h after the TBS. Scale bars: 5 mV/5 ms. (F) During the induction protocol, granule cells tended to fire "bursts" of action potentials, especially after the second repetition of the theta-burst stimulation protocol, as illustrated in the representative traces (upper traces: wild-type slice), whereas the Cav3.2 knockouts were much more reluctant to it (lower traces: Cav3.2 knockout). We quantified the ratio of the second population spike amplitude in the burst to the amplitude of the first spike. The burst ratio in wild-type slices (1.07 ± 0.18) significantly differed from the burst ratio in the knockout group (0.32 ± 0.15) ($P < 0.05$, Mann–Whitney U-test). (G) This burst ratio was significantly correlated with the actual amount of synaptic potentiation 1 h later (Spearman coefficient of correlation $r = 0.55$, $P < 0.01$). *$P < 0.05$, Mann–Whitney U-test.

confirming the intact basal excitability of mature granule cells lacking Cav3.2 channels (Supplementary Fig. S4C). However, a major difference was observed in the ability to fire more than one action potential. The field-EPSP slope needed to fire bursts of 2 or 3 action potentials was increased by more than 1.5-fold in knockout animals compared with control values (Supplementary Fig. S4E).

Collectively, the results point to a reduced ability of mature granule cells lacking the Cav3.2 channel to elicit more than one action potential in response to a given synaptic input.

Cav3.2 Knockout Mice Exhibit Reduced Synaptic Plasticity

Next, we searched for possible physiological implications of the impairment in the ability to fire bursts of action potentials in Cav3.2 knockout mice. As it has been shown that postsynaptic bursting is an important element for the induction of synaptic plasticity in hippocampal pyramidal cells (Pike et al. 1999), we

assessed whether that could also be the case for dentate granule cells.

We performed this series of experiments in the absence of bicuculline, with an intact network. A stimulation electrode was placed at the level of the medial perforant path, and 2 recording electrodes were positioned: one at the granule cell layer for population spike recording and another in the middle of the molecular layer to record the field-EPSP. As in previous experiments, the general excitability of dentate granule cells was not significantly changed in basal conditions by the absence of the Cav3.2 channels (Fig. 6A–C). Moreover, the paired pulse ratio (second potential/first potential) for an interstimulus interval of 50 ms was indistinguishable between both genotypes (EPSP ratio: wt 0.93 ± 0.02, ko 0.93 ± 0.01; PSA ratio: wt $2.17.4 \pm 0.24$, ko 2.09 ± 0.24). However, the level of synaptic potentiation elicited by a TBS protocol in knockout slices was significantly reduced compared with the control group (Fig. 6D,E).

To facilitate the bursting of cells, we increased the duration of the stimulus pulse at the time of the induction protocol.
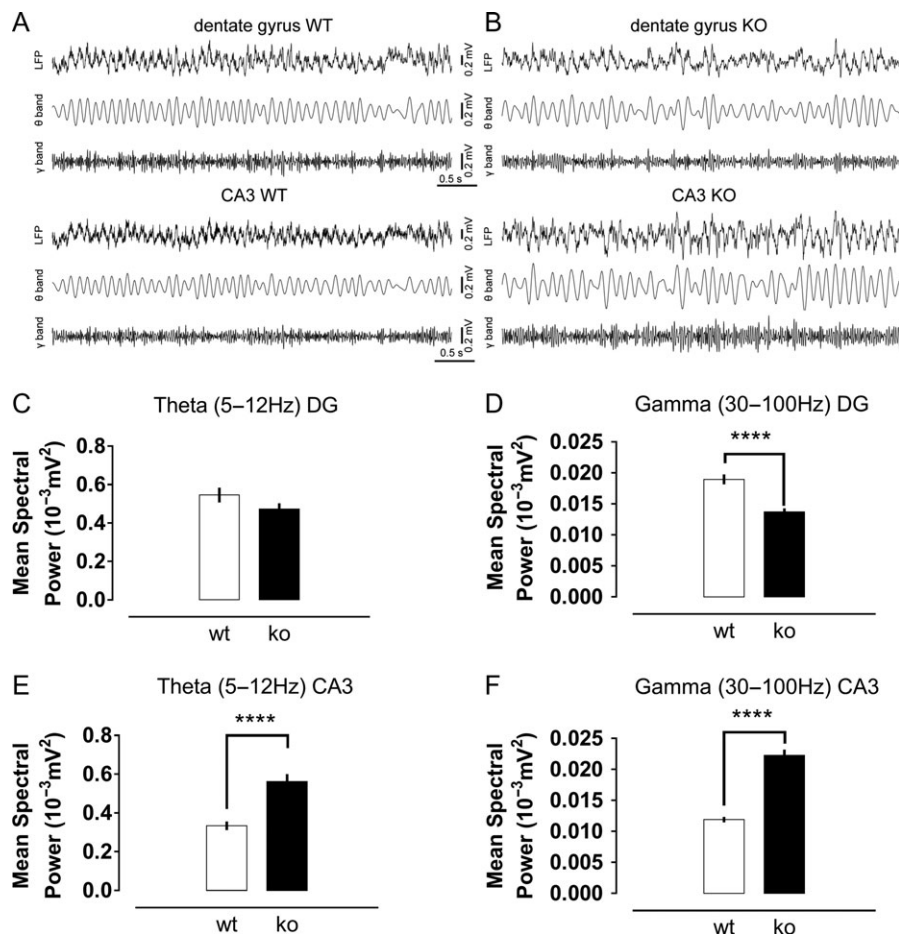
Figure 7. Abnormal oscillatory activity in the dentate gyrus and CA3 area of knockout mice. Representative traces of the local field potential recorded in the dentate gyrus and CA3 of freely behaving wild-type (*A*) and Cav3.2 knockout mice (*B*). Mean power of theta (*C*) and gamma (*D*) oscillations in the dentate gyrus of both experimental groups. Gamma oscillations had a reduced power in the knockout mice. Theta (*E*) and gamma (*F*) oscillations in the CA3 area had higher spectral power in knockout animals. ****$P < 0.0001$, *t*-test.

Interestingly, we observed that this manipulation was quite effective for wild-type granule cells that tended to fire a doublet of action potentials after the first TBS repeat (secondPSA-to-firstPSA average for the repeats 2, 3, and 4 of the TBS: 0.83 ± 0.14). This doublet firing was strongly impaired in the Cav3.2 knockout group (secondPSA-to-firstPSA average for repeats 2, 3, and 4: 0.27 ± 0.10) (Fig. 6F). Furthermore, this "burst-ratio" was significantly correlated with the amount of synaptic potentiation elicited ($R = 0.55$, $P < 0.01$) (Fig. 6G).

Altogether, these results indicate that bursting at the time of plasticity induction is strongly related to the amount of synaptic potentiation elicited in mature granule cells, at least for the TBS. The Cav3.2 knockout mice showed an impairment of their bursting ability that translated into a reduction in the amount of potentiation afterward.

Cav3.2 Knockout Mice Show Disturbed Hippocampal Oscillations, Impaired Dentate Granule Cell Burst Firing and Decreased CA3 Spiking Activity In Vivo

We were next interested to assess whether the observed impairment in the bursting capability of mature granule cells had further implications in hippocampal physiology, particularly in the firing of the CA3 postsynaptic targets. To this end, we implanted tetrodes into the dentate and CA3 of wild-type

and knockout animals to record LFPs and single unit activity from these hippocampal regions in awake animals during exploration of a new context.

We observed that both theta and gamma rhythms were significantly disturbed in the absence of Cav3.2 channels. Knockout mice did not show prominent changes in the power of the theta oscillations in the dentate gyrus, but a significant reduction in the power of gamma oscillations (Fig. 7C,D). For CA3, significant increases in both theta and gamma oscillation power were detected (Fig. 7E,F). A second interesting observation was the confirmation of an impairment of the burst firing in the dentate gyrus of knockout mice in vivo. The mean firing rate and, especially, the mean bursting rate were significantly diminished in the knockout group (Fig. 8A,B). To better understand this finding, we further quantified the frequency of "event" rate, considering an event as the occurrence of either a single action potential or a burst of action potentials. The reasoning for this quantification is that the mean firing rate might be affected by the number of bursts. In addition, as we expected a reduction in the number of bursts in knockout animals according to our in vitro data, this could explain the lower firing rate in this group. Interestingly, despite a trend to lower values in the knockouts, the mean event rate was not significantly different between groups (Fig. 8C), suggesting a mild or absent influence of Cav3.2 channels on the general excitability of
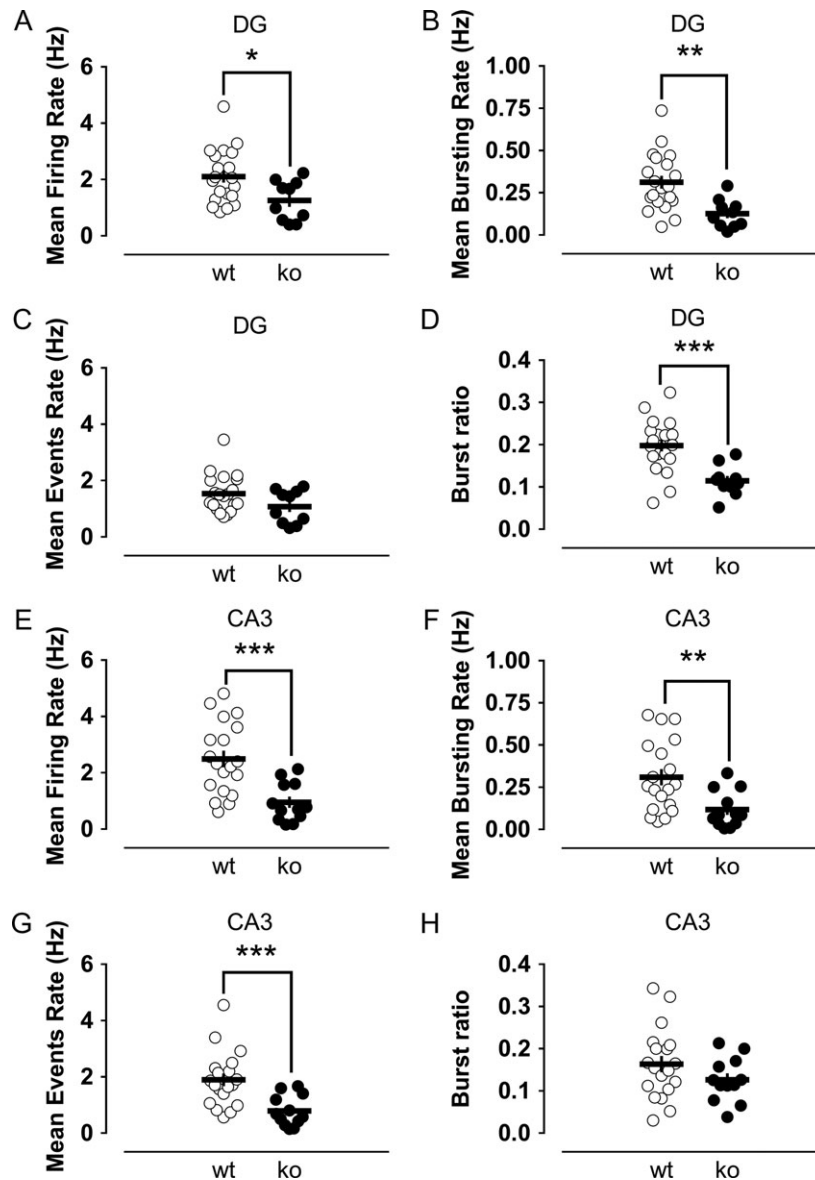
Figure 8. Impaired burst firing capability in the dentate gyrus of Cav3.2 knockout mice with concomitantly reduced CA3 activity suggests a compromised dentate-to-CA3 communication in the absence of the Cav3.2 channels. The mean firing rate (A) and mean bursting rate (B) were significantly reduced in the dentate gyrus of knockouts. The similar mean event rates (C) between the groups and the reduced burst ratio (D) of the knockout mice showed an impairment in the bursting capability of putative granule cells lacking the Cav3.2 channel, with no big changes in general excitability. Regarding the CA3 area, the mean firing rate (E), mean bursting rate (F) and mean event rate (G) were significantly decreased in comparison to the rates in the control group. As the burst ratio in knockouts was similar to that in controls (H), the results showed that the impairment in the firing rate of CA3 was related to the impaired dentate bursting ability. *,**,***$P < 0.05$, $P < 0.01$ and $P < 0.001$, Mann–Whitney U-test.

granule cells. However, the most remarkable observation was that the proportion of bursts from the total number of events in wild-type mice was twice that measured in the knockouts (Fig. 8D). This reduction in the frequency of bursts in the dentate of knockout animals was concomitant with a highly significant drop in the mean firing rate and mean event rate in the CA3 region (Fig. 8E–G), consistent with the importance of the burst firing of granule cells for the effective triggering of their postsynaptic CA3 targets.

Discussion

Burst firing in the dentate gyrus has often been associated with pathological conditions such as epilepsy (Shao and Dudek 2011;

Dengler and Coulter 2016; Kelly and Beck 2017). However, recent in vivo recordings have shown that mature granule cells preferentially fire in bursts while animals are exploring a new environment (Pernía-Andrade and Jonas 2014). Bursts of action potentials should have a particularly crucial role for neurons that otherwise mainly remain silent and even more so for granule cells, whose synapses with their CA3 pyramid targets exhibit one of the strongest short-term facilitations known in central synapses (Nicoll and Schmitz 2005).

The bursting phenotype we described here correlates well with the kinetic properties of the T-type calcium channels, which quickly inactivate afterdepolarization and can therefore preferentially affect the earliest spikes in the discharge (Perez-Reyes 2003). Indeed, reducing T-type channel activity by means of
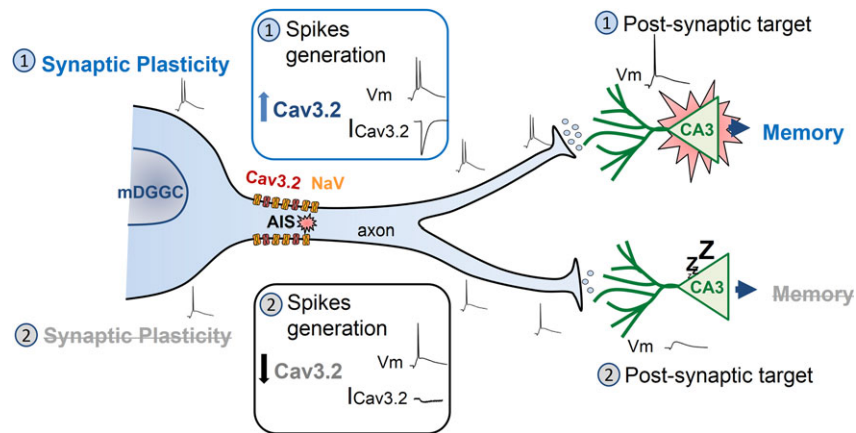
Figure 9. Proposed model of the Cav3.2 channel as a critical switch for mature granule cells to support synaptic plasticity and be effective in transmitting information to the CA3 pyramids. A schematic mature granule cell sending axonal projections to CA3 pyramidal neurons, representing 2 different conditions of Cav3.2 channel activity. *Top half*: Cav3.2 current ($I_{Cav3.2}$) enhances the ability of mature granule cells to generate high-frequency bursts of action potentials. This process, in turn, facilitates synaptic plasticity in the proper granule cells and produces a sufficiently strong stimulation of the postsynaptic CA3 pyramidal neurons to initiate spikes. *Bottom half*: low numbers of Cav3.2 channels or downregulation of their activity results in a reduced $I_{Cav3.2}$. As a consequence, mature granule cells are impaired in their ability to produce action potential bursts. This translates to reduced synaptic plasticity and inefficient stimulation of postsynaptic CA3 pyramidal cells.

of pharmacological blockers impaired the burst firing of mature granule cells. However, as previously reported (Schmidt-Hieber et al. 2004; Martinello et al. 2015), we did not observe significant changes in the general excitability of mature granule cells after T-type channel blockade. Furthermore, we found that the effect of T-type channels on bursting is mediated by axonal T-type channels, presumably in the AIS, a structure of crucial importance in the generation of the action potential (Buffington and Rasband 2011; Bender and Trussell 2012; Yamada and Kuba 2016). Due to the low conductance of T-type channels and their consequently confined effects, T-type channel localization at key targets such as the AIS might significantly contribute to potentiate their action. Notably, the AIS of granule cells shows structural and functional plasticity (Regehr and Tank 1991; Evans et al. 2013; Scott et al. 2014; Martinello et al. 2015), from a distal shifting of the whole AIS in response to prolonged neuronal activity (Evans et al. 2013) to submillisecond distance-dependent inactivation of sodium channels depending on the kinetics of the ongoing depolarization (Scott et al. 2014).

T-type channels comprise 3 family members, Cav3.1, Cav3.2 and Cav3.3, which differ in their molecular structure, voltage-dependence and kinetic properties (Perez-Reyes 2003). Cav3.2 is found all along the granule cell membrane, including the AIS (Martinello et al. 2015; Aguado et al. 2016). Moreover, animals lacking this channel isoform have deficits in hippocampal-dependent learning (Chen et al. 2012; Gangarossa et al. 2014). We therefore hypothesized that Cav3.2 might be the key player in controlling the burst firing of mature granule cells. We found that Cav3.2 knockout animals were severely impaired in their ability to fire bursts of action potentials in vitro in spite of an otherwise similar excitability compared with that of controls. This impairment in burst firing resulted in reduced synaptic plasticity properties in knockout mice, which exhibited roughly half of the potentiation levels of wild-type animals. Bursts of action potentials can backpropagate to dendrites better than single action potentials can, allowing stronger local depolarization and a larger calcium influx in dendrites and synapses, thereby facilitating the induction of synaptic plasticity (Pike et al. 1999; Buzsáki et al. 2002). Bursts could also produce a larger increase in calcium in the soma, potentially influencing transcription and translation processes. We aimed to further

assess physiological consequences of the absence of Cav3.2 in vivo and recorded LFPs and single unit activity from the dentate gyrus and CA3 of knockout and control awake mice. Knockout animals had disrupted oscillatory activity in both the dentate and CA3 area. An interesting finding was the reduction in the power of gamma oscillations in the dentate gyrus and a concomitant increase in CA3. Why the dentate gamma power was decreased in Cav3.2 knockout animals is not completely clear, but the impairment in burst firing of granule cells might be an important contributing factor. Two main generators of gamma oscillations in the hippocampus are the dentate gyrus and the CA3 region (Csicsvari et al. 2003; Colgin and Moser 2010). A reduction in the power of the gamma oscillations in the dentate has been shown to lead to a compensatory increase in the activity of the CA3 generator (Bragin et al. 1995; Csicsvari et al. 2003; Montgomery et al. 2008), similar to what we found. We also recorded single unit activity and observed a significant impairment in the bursting rate of putative granule cells of Cav3.2 knockout mice in vivo. Most importantly, this reduction in the bursting capability of granule cells was accompanied by a strong reduction in the mean firing frequency of CA3 cells, without any significant effects on bursting in this region. These findings suggest different mechanisms that support bursting in granule cells compared with pyramidal cells. Furthermore, they are consistent with the importance of granule cell bursting for the triggering of postsynaptic CA3 targets. However, these results should be cautiously interpreted, as the Cav3.2 knockouts are a constitutive global Cav3.2 knockout strain lacking the channel in all cells—including the CA3 pyramidal cells for which an important role of T-type channels in neuronal excitability has been suggested (Reid et al. 2008)—during their life-spans. However, together with published behavioral data (Chen et al. 2012; Gangarossa et al. 2014), our study points to the critical role of Cav3.2-mediated cell bursting for the formation and/or retrieval of hippocampal-dependent memories.

Blockade of T-type calcium channels in the AIS significantly modifies both the general excitability and the bursting ability of dorsal cochlear nucleus interneurons (Bender and Trussell 2009). Here, we described mostly a specific modulatory effect of Cav3.2 on bursting, and not on firing per se, under basal conditions. However, our results do not preclude the possibility of an

effect on general excitability in other circumstances. T-type calcium channels were recently shown to be present at the AIS of mature granule cells, where by modulating the M-type potassium channels, they can modify the action potential threshold (Martinello et al. 2015). In that study, however, only changes in action potential threshold were evaluated, with no assessment of the bursting ability of mature granule cells. Moreover, such effects on the action potential threshold were only seen when T-type channel functionality was potentiated through cholinergic stimulation. However, no effects on threshold or other modifications were reported after T-type channel blockade in the basal state (Martinello et al. 2015). Thus, no function of T-type channels in basal physiological conditions similar to in the present work has been described for mature granule cells. Collectively our data suggest that T-type channels in mature granule cells indeed play a crucial role in basal conditions by supporting the ability of these neurons to fire bursts of action potentials, which is in turn important for synaptic plasticity and proper dentate-to-CA3 communication. We therefore propose that Cav3.2 channels could act as a switch for mature granule cells (Fig. 9). By controlling their ability to fire bursts of action potentials, Cav3.2 channels might determine to which extent mature granule cells will undergo synaptic plasticity and how effective they will be in transmitting information to the CA3 pyramids. In this context, neuromodulation could be a powerful way through which mature granule cell bursting and dentate-to-CA3 communication might be effectively fine-tuned, as T-type channels are known to be regulated by many important neurotransmitters and hormones (Perez-Reyes 2003). Thus, we propose that due to the low basal excitability of mature granule cells, their bursting capability is a crucial element for their physiological function.

Supplementary Material

Supplementary material is available at *Cerebral Cortex* online.

Authors' Contributions

M.D., O.S., A.D., M.R.K., M.H., A.B., and J.L.-R. designed the research; M.D., O.S., A.M., and J.L.-R. performed the research; M.D., A.B., and J.L.-R. analyzed the data; and M.D., A.B., and J.L.-R. wrote the article. M.D., O.S., E.B., A.D., M.R.K., M.H., A.B., and J.L.-R. edited the text and figures, providing important intellectual content.

Funding

Notes

References

Aguado C, García-Madrona S, Gil-Minguez M, Luján R. 2016. Ontogenic changes and differential localization of T-type Ca2+ channel subunits Cav3.1 and Cav3.2 in mouse hippocampus and cerebellum. Front Neuroanat. 10:83.

Alme CB, Buzzetti RA, Marrone DF, Leutgeb JK, Chawla MK, Schaner MJ, Bohanick JD, Khoboko T, Leutgeb S, Moser EI, et al. 2010. Hippocampal granule cells opt for early retirement. Hippocampus. 20(10):1109–1123.

Bender KJ, Trussell LO. 2009. Axon initial segment Ca^{2+} channels influence action potential generation and timing. Neuron. 61(2):259–271.

Bender KJ, Trussell LO. 2012. The physiology of the axon initial segment. Annu Rev Neurosci. 35:249–265.

Bijlenga P, Liu J-H, Espinos E, Haenggeli C-A, Fischer-Lougheed J, Bader CR, Bernheim L. 2000. T-type α1H Ca^{2+} channels are involved in Ca^{2+} signaling during terminal differentiation (fusion) of human myoblasts. Proc Natl Acad Sci USA. 97(13): 7627–7632.

Blaxter TJ, Carlen PL, Niesen C. 1989. Pharmacological and anatomical separation of calcium currents in rat dentate granule neurones *in vitro*. J Physiol. 412:93–112.

Bourinet E, Stotz SC, Spaetgens RL, Dayanithi G, Lemos J, Nargeot J, Zamponi GW. 2001. Interaction of SNX482 with domains III and IV inhibits activation gating of alpha(1E) (Ca (V)2.3) calcium channels. Biophys J. 81(1):79–88.

Bragin A, Jando G, Nadasdy Z, Hetke J, Wise K, Buzsaki G. 1995. Gamma (40–100 Hz) oscillation in the hippocampus of the behaving rat. J Neurosci. 15(1):47–60.

Breustedt J, Vogt KE, Miller RJ, Nicoll RA, Schmitz D. 2003. α1E-Containing Ca2+ channels are involved in synaptic plasticity. Proc Natl Acad Sci USA. 100(21):12450–12455.

Buffington SA, Rasband MN. 2011. The axon initial segment in nervous system disease and injury. Eur J Neurosci. 34(10): 1609–1619.

Buzsáki G, Csicsvari J, Dragoi G, Harris K, Henze D, Hirase H. 2002. Homeostatic maintenance of neuronal excitability by burst discharges *in vivo*. Cereb Cortex. 12(9):893–899.

Chen C-C, Lamping KG, Nuno DW, Barresi R, Prouty SJ, Lavoie JL, Cribbs LL, England SK, Sigmund CD, Weiss RM, et al. 2003. Abnormal coronary function in mice deficient in alpha1H T-type Ca2+ channels. Science. 302(5649): 1416–1418.

Chen C-C, Shen J-W, Chung N-C, Min M-Y, Cheng S-J, Liu IY. 2012. Retrieval of context-associated memory is dependent on the Cav3.2 T-type calcium channel. PLoS One. 7(1):e29384.

Colgin LL, Moser EI. 2010. Gamma oscillations in the hippocampus. Physiology (Bethesda). 25(5):319–329.

Csicsvari J, Jamieson B, Wise KD, Buzsáki G. 2003. Mechanisms of gamma oscillations in the hippocampus of the behaving rat. Neuron. 37(2):311–322.

Cui Y, Liu X, Yang T, Mei Y-A, Hu C. 2014. Exposure to extremely low-frequency electromagnetic fields inhibits T-type calcium channels via AA/LTE4 signaling pathway. Cell Calcium. 55(1):48–58.

Debanne D, Campanac E, Bialowas A, Carlier E, Alcaraz G. 2011. Axon physiology. Physiol Rev. 91(2):555–602.

Dengler CG, Coulter DA. 2016. Normal and epilepsy-associated pathologic function of the dentate gyrus. Prog Brain Res. 226:155–178.

Dieni CV, Nietz AK, Panichi R, Wadiche JI, Overstreet-Wadiche L. 2013. Distinct determinants of sparse activation during granule cell maturation. J Neurosci. 33(49):19131–19142.

Engbers JDT, Anderson D, Asmara H, Rehak R, Mehaffey WH, Hameed S, McKay BE, Kruskic M, Zamponi GW, Turner RW. 2012. Intermediate conductance calcium-activated potassium channels modulate summation of parallel fiber input in cerebellar Purkinje cells. Proc Natl Acad Sci USA. 109(7): 2601–2606.

Evans MD, Sammons RP, Lebron S, Dumitrescu AS, Watkins TBK, Uebele VN, Renger JJ, Grubb MS. 2013. Calcineurin signalling mediates activity-dependent relocation of the axon initial segment. J Neurosci. 33(16):6950–6963.

Fernández JA, McGahon MK, McGeown JG, Curtis TM. 2015. CaV3.1 T-type Ca^{2+} channels contribute to myogenic signaling in rat retinal arterioles. Invest Ophthalmol Vis Sci. 56(9): 5125–5132.

Francois A, Kerckhove N, Meleine M, Alloui A, Barrere C, Gelot A, Uebele VN, Renger JJ, Eschalier A, Ardid D, et al. 2013. State-dependent properties of a new T-type calcium channel blocker enhance Ca(V)3.2 selectivity and support analgesic effects. Pain. 154(2):283–293.

Gabso M, Neher E, Spira ME. 1997. Low mobility of the Ca2+ buffers in axons of cultured Aplysia neurons. Neuron. 18(3): 473–481.

Gangarossa G, Laffray S, Bourinet E, Valjent E. 2014. T-type calcium channel Cav3.2 deficient mice show elevated anxiety, impaired memory and reduced sensitivity to psychostimulants. Front Behav Neurosci. 8:92.

Ge S, Yang CH, Hsu KS, Ming GL, Song H. 2007. A critical period for enhanced synaptic plasticity in newly generated neurons of the adult brain. Neuron. 54(4):559–566.

Henze DA, Wittner L, Buzsáki G. 2002. Single granule cells reliably discharge targets in the hippocampal CA3 network in vivo. Nat Neurosci. 5(8):790–795.

Huang L, Keyser BM, Tagmose TM, Hansen JB, Taylor JT, Zhuang H, Zhang M, Ragsdale DS, Li M. 2004. NNC 55-0396 [(1S,2S)-2-(2-(N-[(3-benzimidazol-2-yl)propyl]-N-methylamino)ethyl)-6-fluoro-1,2,3,4-tetrahydro-1-isopropyl-2-naphtyl cyclopropanecarboxylate dihydrochloride]: a new selective inhibitor of T-type calcium channels. J Pharmacol Exp Ther. 309(1):193–199.

Iftinca M, McKay BE, Snutch TP, McRory JE, Turner RW, Zamponi GW. 2006. Temperature dependence of T-type calcium channel gating. Neuroscience. 142(4):1031–1042.

Joksovic PM, Bayliss DA, Todorovic SM. 2005. Different kinetic properties of two T-type Ca2+ currents of rat reticular thalamic neurones and their modulation by enflurane. J Physiol. 566(Pt 1):125–142.

Kelly T, Beck H. 2017. Functional properties of granule cells with hilar basal dendrites in the epileptic dentate gyrus. Epilepsia. 58(1):160–171.

Kesner RP, Rolls ET. 2015. A computational theory of hippocampal function, and tests of the theory. Neurosci Biobehav Rev. 48:92–147.

Kimm T, Bean BP. 2014. Inhibition of A-type potassium current by the peptide toxin SNX-482. J Neurosci. 34(28):9182–9189.

Kraus RL, Li Y, Gregan Y, Gotter AL, Uebele VN, Fox SV, Doran SM, Barrow JC, Yang Z-Q, Reger TS, et al. 2010. In vitro characterization of T-type calcium channel antagonist TTA-A2 and in vivo effects on arousal in mice. J Pharmacol Exp Ther. 335(2):409–417.

Krueppel R, Remy S, Beck H. 2011. Dendritic integration in hippocampal dentate granule cells. Neuron. 71(3):512–528.

Lee JH, Gomora JC, Cribbs LL, Perez-Reyes E. 1999. Nickel block of three cloned T-type calcium channels: low concentrations selectively block alpha1H. Biophys J. 77(6):3034–3042.

Li M, Hansen JB, Huang L, Keyser BM, Taylor JT. 2005. Towards selective antagonists of T-type calcium channels: design, characterization and potential applications of NNC 55-0396. Cardiovasc Drug Rev. 23(2):173–196.

Lopez-Rojas J, Kreutz MR. 2016. Mature granule cells of the dentate gyrus—passive bystanders or principal performers in hippocampal function? Neurosci Biobehav Rev. 64: 167–174.

Ly R, Bouvier G, Szapiro G, Prosser HM, Randall AD, Kano M, Sakimura K, Isope P, Barbour B, Feltz A. 2016. Contribution of postsynaptic T-type calcium channels to parallel fibre-Purkinje cell synaptic responses. J Physiol. 594(4):915–936.

Martin RL, Lee JH, Cribbs LL, Perez-Reyes E, Hanck DA. 2000. Mibefradil block of cloned T-type calcium channels. J Pharmacol Exp Ther. 295(1):302–308.

Martinello K, Huang Z, Lujan R, Tran B, Watanabe M, Cooper EC, Brown DA, Shah MM. 2015. Cholinergic afferent stimulation induces axonal function plasticity in adult hippocampal granule cells. Neuron. 85(2):346–363.

McDonough SI, Bean BP. 1998. Mibefradil inhibition of T-type calcium channels in cerebellar purkinje neurons. Mol Pharmacol. 54(6):1080–1087.

Metz AE, Jarsky T, Martina M, Spruston N. 2005. R-type calcium channels contribute to afterdepolarization and bursting in hippocampal CA1 pyramidal neurons. J Neurosci. 25(24): 5763–5773.

Mongiat LA, Esposito MS, Lombardi G, Schinder AF. 2009. Reliable activation of immature neurons in the adult hippocampus. PLoS One. 4(4):e5320.

Montgomery SM, Sirota A, Buzsáki G. 2008. Theta and gamma coordination of hippocampal networks during waking and rapid eye movement sleep. J Neurosci. 28(26):6731–6741.

Newcomb R, Szoke B, Palma A, Wang G, Chen XH, Hopkins W, Cong R, Miller J, Urge L, Tarczy-Hornoch K, et al. 1998. Selective peptide antagonist of the class E calcium channel from the venom of the tarantula Hysterocrates gigas. Biochemistry. 37(44):15353–15362.

Nicoll RA, Schmitz D. 2005. Synaptic plasticity at hippocampal mossy fibre synapses. Nat Rev Neurosci. 6(11):863–876.

Obejero-Paz CA, Gray IP, Jones SW. 2008. Ni2+ block of CaV3.1 (alpha1G) T-type calcium channels. J Gen Physiol. 132(2): 239–250.

Paxinos G, Franklin KBJ. 2012. Paxinos and Franklin's the mouse brain in stereotaxic coordinates. 4th ed. Amsterdam: Academic Press. p. 360.

Perez-Reyes E. 2003. Molecular physiology of low-voltage-activated T-type calcium channels. Physiol Rev. 83(1): 117–161.

Pernía-Andrade AJ, Jonas P. 2014. Theta-gamma-modulated synaptic currents in hippocampal granule cells in vivo define a mechanism for network oscillations. Neuron. 81(1): 140–152.

Pike FG, Meredith RM, Olding AW, Paulsen O. 1999. Rapid report. J Physiol. 518(Pt 2):571–576.

Pourbadie HG, Naderi N, Delavar HM, Hosseinzadeh M, Mehranfard N, Khodagholi F, Janahmadi M, Motamedi F. 2017. Decrease of high voltage Ca(2+) currents in the dentate gyrus granule cells by entorhinal amyloidopathy is reversed by calcium channel blockade. Eur J Pharmacol. 794:154–161.

Regehr WG, Tank DW. 1991. The maintenance of LTP at hippocampal mossy fiber synapses is independent of sustained presynaptic calcium. Neuron. 7(3):451–459.

Reid CA, Xu S, Williams DA. 2008. Spontaneous release from mossy fiber terminals inhibits Ni2+-sensitive T-type Ca2+

channels of CA3 pyramidal neurons in the rat organotypic hippocampal slice. Hippocampus. 18(7):623–630.

Sabatini BL, Oertner TG, Svoboda K. 2002. The life cycle of Ca(2+) ions in dendritic spines. Neuron. 33(3):439–452.

Sajikumar S, Navakkode S, Frey JU. 2005. Protein synthesis-dependent long-term functional plasticity. Curr Opin Neurobiol. 15(5):607–613.

Schmidt-Hieber C, Bischofberger J. 2010. Fast sodium channel gating supports localized and efficient axonal action potential initiation. J Neurosci. 30(30):10233–10242.

Schmidt-Hieber C, Jonas P, Bischofberger J. 2004. Enhanced synaptic plasticity in newly generated granule cells of the adult hippocampus. Nature. 429(6988):184–187.

Scott RS, Henneberger C, Padmashri R, Anders S, Jensen TP, Rusakov DA. 2014. Neuronal adaptation involves rapid expansion of the action potential initiation site. Nat Commun. 5:3817.

Senkov O, Mironov A, Dityatev A. 2015. A novel versatile hybrid infusion-multielectrode recording (HIME) system for acute drug delivery and multisite acquisition of neuronal activity in freely moving mice. Front Neurosci. 9:425.

Senkov O, Mironov A, Dityatev A. 2016. An advanced 3D printed design of the hybrid infusion-multielectrode recording system for local field potential and single unit acquisition and intrabrain drug delivery in freely moving mice. Med Technol Med. 8(4):129–132.

Shao L-R, Dudek FE. 2011. Repetitive perforant-path stimulation induces epileptiform bursts in minislices of dentate gyrus from rats with kainate-induced epilepsy. J Neurophysiol. 105(2):522–527.

Sochivko D, Pereverzev A, Smyth N, Gissel C, Schneider T, Beck H. 2002. The CaV2.3 Ca2+ channel subunit contributes to R-Type Ca2+ currents in murine hippocampal and neocortical neurones. J Physiol. 542(Pt 3):699–710.

Staley KJ, Otis TS, Mody I. 1992. Membrane properties of dentate gyrus granule cells. J Neurophysiol. 67(5):1346–1358.

Temprana SG, Mongiat LA, Yang SM, Trinchero MF, Alvarez DD, Kropff E, Giacomini D, Beltramone N, Lanuza GM, Schinder AF. 2015. Delayed coupling to feedback inhibition during a critical period for the integration of adult-born granule cells. Neuron. 85(1):116–130.

Todorovic SM, Jevtovic-Todorovic V. 2011. T-type voltage-gated calcium channels as targets for the development of novel pain therapies. Br J Pharmacol. 163(3):484–495.

Todorovic SM, Jevtovic-Todorovic V, Meyenburg A, Mennerick S, Perez-Reyes E, Romano C, Olney JW, Zorumski CF. 2001. Redox modulation of T-type calcium channels in rat peripheral nociceptors. Neuron. 31(1):75–85.

Wang S, Scott BW, Wojtowicz JM. 2000. Heterogenous properties of dentate granule neurons in the adult rat. J Neurobiol. 42(2):248–257.

Weiss N, Zamponi GW. 2013. Control of low-threshold exocytosis by T-type calcium channels. Biochim Biophys Acta. 1828 (7):1579–1586.

Yamada R, Kuba H. 2016. Structural and functional plasticity at the axon initial segment. Front Cell Neurosci. 10:250.

Yamamoto Y, Fukuta H, Suzuki H. 1993. Blockade of sodium channels by divalent cations in rat gastric smooth muscle. Jpn J Physiol. 43(6):785–796.

Yasuda R, Nimchinsky EA, Scheuss V, Pologruto TA, Oertner TG, Sabatini BL, Svoboda K. 2004. Imaging calcium concentration dynamics in small neuronal compartments. Sci STKE. 2004(219):pl5.

Zhang L, Valiante TA, Carlen PL. 1993. Contribution of the low-threshold T-type calcium current in generating the post-spike depolarizing afterpotential in dentate granule neurons of immature rats. J Neurophysiol. 70(1):223–231.